

Numerical Modelling of Heat and Mass Transfer in Porous Materials During Drying and Shrinkage

D. Lelièvre^{*1}, V. Nicolas¹, P. Glouannec¹, J.P Ploteau¹

¹Université de Bretagne-Sud, Laboratoire d'Ingénierie des MATériaux de Bretagne – Equipe Thermique et Energétique

Dylan Lelièvre : Université de Bretagne Sud, Centre de Recherche- BP92116, 56321 LORIENT CEDEX France, dylan.lelievre@univ-ubs.fr

Abstract : In this paper, we present a model allowing to properly simulate the pressure, heat and mass transfer during the drying of moist plaster on dry concrete. We take advantage of the continuity of vapour pressure between two materials to use it as the main variable in the mass conservation equation, and calculate the moisture content separately through a partial differential equation. This model will also integrate the deformation of plaster.

Keywords : moisture content, temperature, pressure, multi-layer wall, building materials.

1. Introduction

Drying is an essential step in many processes, for it will have an important impact on the product quality and energy consumption. Many numerical models have been realised over decades, in order to predict the hygrothermal behaviour of porous media during the drying process, depending on external parameters such as air temperature, relative humidity and velocity. And, in certain cases, the shrinkage must not be neglected.

Most of these models use three variables : moisture content, temperature and pressure while complete enough to simulate the behaviour of a single-layer system. This kind of model shows its limits when applied to a multilayered wall; the discontinuity of moisture content at the interface will cause numerical errors and insoluble equations.

In this study the objective is to simulate the drying phase of a plaster applied on a wall. Firstly, the governing equations and the materials properties are presented. Then numerical model is described. Simulating results show the influence of the initial temperature of each material.

2. Governing equations

The hygrothermal behaviour of a two-layer wall described in the figure 1 is studied. Temperature T , vapour pressure P_v and total pressure of the gaseous phase P_g are calculated by a numerical model. For the heat and mass transfer, the physical model is based on the approach developed by De Vries[1,2] and Whitaker [3].

At the interface between the two layers, the works of Tariku[4] and Oin[5] are used..

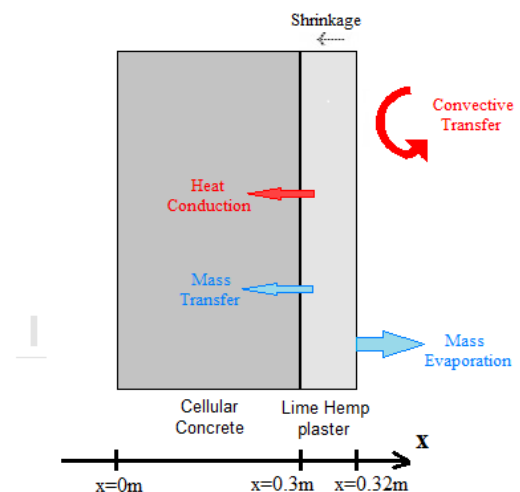


Figure 1 : Description of the modeled system

2.1 Hypothesis

The model used for heat and mass transfers follows the macroscopic approach developed by Salagnac[6].

Moreover, one assumes that :

- the system is one-dimensional,
- the liquid phase is not compressible ($\rho_l = \text{constant}$)
- the effect of gravity is neglected,
- the shrinkage of dry concrete is neglected,
- no chemical reactions occur within the material,
- the gaseous phase consists of a perfect blend of gas : dry air (a) and vapour (v), following the equations $P_g = P_a + P_v$ and

$$\rho_g = \rho_a + \rho_v$$

2.2 Mass conservation

We use the equations derived from the Fick law from diffusion and Darcy's generalised equations giving the mean filtration velocity fields of the liquid and gaseous phases.

$$\text{Liquid water : } \frac{\partial \rho_l}{\partial t} + \nabla(\rho_l V_l) = -K \quad (1)$$

$$\text{Vapour water : } \frac{\partial \rho_v}{\partial t} + \nabla(\rho_v V_v) = K \quad (2)$$

$$\text{Air : } \frac{\partial \rho_a}{\partial t} + \nabla(\rho_a V_a) = 0 \quad (3)$$

with K the phase change rate given by the relation

$$K = \nabla(D_v^T \nabla T + D_v^W \nabla W + D_v^{Pg} \nabla P_g) \quad (4)$$

We write the expressions of the mass flux on the form :

Liquid water flux :

$$\rho_l V_l = D_l^T \nabla T + D_l^W \nabla W \quad (5)$$

Vapour water flux :

$$\rho_v V_v = D_v^T \nabla T + D_v^W \nabla W \quad (6)$$

Air flux :

$$\rho_a V_a = D_a^T \nabla T + D_a^W \nabla W \quad (7)$$

In these relations, W is the moisture content, given by the fraction between the water mass and the dried solid mass :

$$W = \frac{m_l}{m_s}$$

and D_l, D_v, D_a are the mass transfer coefficients calculated in the appendix.

Shrinkage

As the media are considered as compressible, we will adapt the time derivative for each variable by adding a velocity term :

$$\left(\frac{\partial i}{\partial t} \right) \rightarrow \left(\frac{\partial i}{\partial t} + \bar{u} \bar{\nabla} i \right) \quad (8)$$

for $i=(W, T, P_g, P_v)$, \bar{u} being the velocity vector within the material.

The velocity u is calculated with the Navier-Stokes Weakly Compressible equation :

$$\frac{\partial \rho_s^{app}}{\partial t} + \nabla(\rho_s^{app} u) = 0 \quad (9)$$

Moisture content equation

By summing the equations (1) and (2), applying the expressions of water flux in the equations (5) and (6) and including the velocity term from (8), we obtain the equation :

$$\rho_s \left(\frac{\partial W}{\partial t} + u \nabla W \right) + \nabla \left[\begin{array}{l} (D_l^W + D_v^W) \nabla W \\ + (D_l^T + D_v^T) \nabla T \\ + (D_l^{Pg} + D_v^{Pg}) \nabla P_g \end{array} \right] = 0 \quad (10)$$

Vapour pressure equation

Because moisture content is discontinued at the interface between two materials, we will change the moisture content equation to use the vapour pressure as a variable, using the formula given by F.Tariku [6] :

$$\partial W = \frac{\theta(W)}{P_{v,sat}} \partial P_v \quad (11)$$

$\theta(W)$ being the sorption capacity (slop of sorption-moisture retention curve) and $P_{v,sat}$ being the saturated vapour pressure of water.

The equation (10) becomes :

$$\frac{\rho_s}{P_{v,sat}} \theta \left(\frac{\partial P_v}{\partial t} + u P_v \right) + \nabla \left[\begin{array}{l} \frac{\theta}{P_{v,sat}} (D_l^W + D_v^W) \nabla P_v \\ + (D_l^T + D_v^T) \nabla T \\ + (D_l^{Pg} + D_v^{Pg}) \nabla P_g \end{array} \right] = 0 \quad (12)$$

Air pressure equation

Mass balance on air gives us the pressure equation :

$$\left(\frac{\partial P_g}{\partial t} + u \nabla P_g \right) = - \frac{1}{\gamma_3} \left[\begin{array}{l} \nabla(D_a^W \nabla W \\ + D_a^T \nabla T + D_a^{Pg} \nabla P_g) \end{array} \right] + \gamma_1 \left(\frac{\partial T}{\partial t} \right) + \gamma_2 \left(\frac{\partial W}{\partial t} \right) \quad (13)$$

γ_1, γ_2 and γ_3 being defined in the appendix.

2.3 Energy conservation

Energy balance is calculated through conductive and convective transfers as well as phase changes :

$$\rho C_p \left(\frac{\partial T}{\partial t} + u \nabla T \right) + D_h \nabla T - \nabla(\lambda \nabla T) + K(L_v + \Delta H_{ad}) = 0 \quad (14)$$

$$\rho C_p = \rho_s (C_{p,s} + W C_{p,l}) \quad (15)$$

$$D_h = \left[\begin{array}{l} (D_l^W \nabla W + D_l^T \nabla T) C_{p,l} \\ + (D_a^W \nabla W + D_a^T \nabla T) C_{p,a} \\ + (D_v^W \nabla W + D_v^T \nabla T) C_{p,v} \end{array} \right] \quad (16)$$

$$\Delta H_{ad} = - \frac{R}{M_v} \left(\frac{\partial \ln(a_w)}{\partial \left(\frac{1}{T} \right)} \right)_w \quad (17)$$

2.4 Boundaries conditions

At the left side of the concrete wall (Figure 1, $x=0m$) :

- Imposed temperature $T = 30^{\circ}C$
- Imposed relative humidity $RH=50\%$

At the interface between the concrete wall and the plaster ($x=0.3m$) :

- Temperature is continuous

$$T_{concrete} = T_{plaster}$$

- Vapour pressure is continuous

$$P_{v,concrete} = P_{v,plaster}$$

At the interface between the plaster and air ($x=0.32m$) :

- Pressure : $P_g = P_{atm}$
- $-\vec{n} \cdot (\lambda \vec{\nabla} T) = h(T_{air} - T)$ (18)
- Vapour pressure :

$$-\vec{n} \cdot (D_1^w + D_v^w) \frac{\theta}{P_{v,sat}} \vec{\nabla} P_v = F_m \quad (19)$$

with

$$F_m = k_m \left(\frac{P_{atm} M_v}{RT_{film}} \right) \ln \left(1 + \left(\frac{P_{v,surf} - P_{v,inf}}{P_{atm} - P_{v,surf}} \right) \right) \quad (20)$$

The vapour pressure at the surface is obtained by the water activity a_w of plaster :

$$P_{v,surf} = a_w \cdot P_{v,sat} \quad (21)$$

3. Physical properties

The sorption isotherm curves and mass coefficients of cellular concrete and lime hemp plaster are presented in figures 2 and 3[7]. The thermophysical properties are given in table 1.

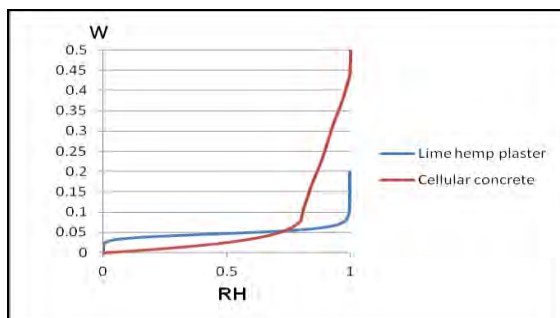


Figure 2 : Sorption isotherm curves of materials

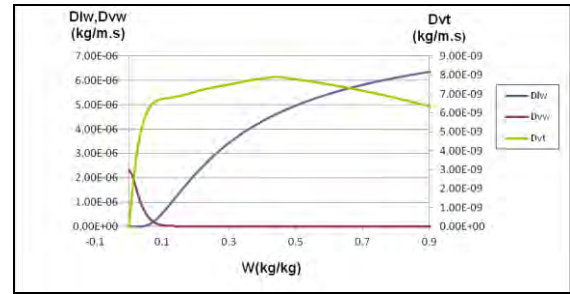


Figure 3.a : Diffusion coefficients of cellular concrete

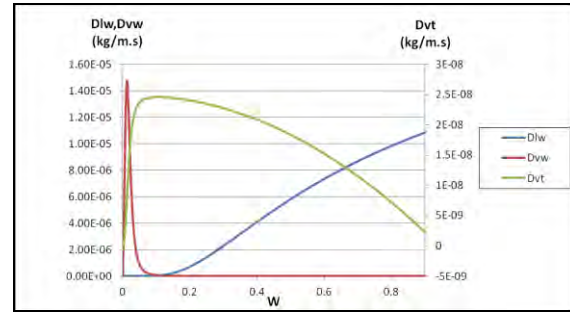


Figure 3.b : Diffusion coefficients of lime hemp plaster

	Cellular concrete	Lime hemp plaster
ρ (kg/m ³)	450	822
Porosity ϵ	0.8	0.65
λ (W/m.K)	$0.15+0.46W$	$0.2038+0.0025W$
C_p (J/K.kg)	840	1040

Table 1 : Thermophysical properties of cellular concrete and lime hemp plaster

4. Results

Firstly we make simulations by calculating only the hygrothermal behaviour of plaster. The idea is to apprehend the influence of the temperature of concrete on the moisture content W and the gas pressure P_g .

In a second phase, we simulate the multi-layer wall.

4.1 Meshing

The system was meshed using a symmetric distribution with a ratio element of 5 in order to have more precise calculations on the interfaces. Each vertical surface only has one element in order to obtain a one-dimensional system. Cellular concrete and lime hemp plaster have respectively 50 and 20 elements (Figure 4).

Besides, a moving mesh ALE was applicated to the plaster layer, in order to modelize the shrinkage calculated with the formula (9), the inside velocity of the mesh being equal to u .

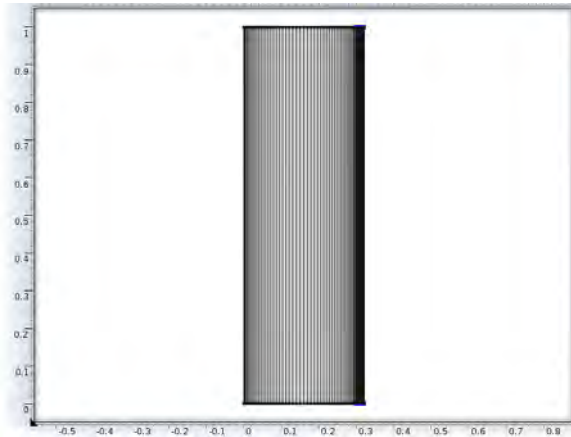


Figure 4.a : Global meshing of the system

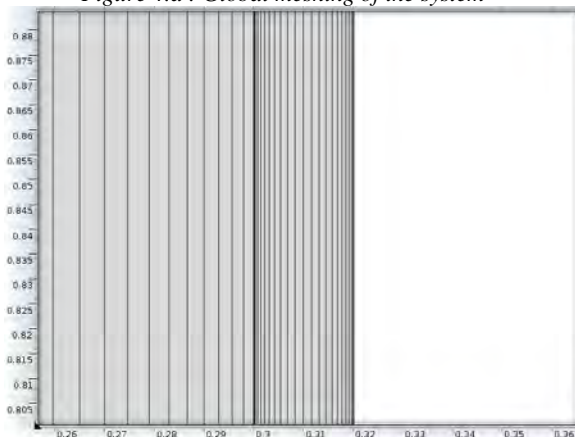


Figure 4.b : Meshing of the plaster layer

4.2 Mono-layer plaster

The initial conditions used are stated in table 2. The following boundary conditions at the interface between concrete and plaster are :

- Imposed temperature $T_b = 30^\circ\text{C}$ or 35°C
- No mass transfer

	Plaster
T(°C)	20
W(kg/kg)	0.69
RH	1

Table 2 : Initial conditions for single-layer simulation

The air has a temperature of 30°C and a relative humidity of 0.5.

The figure 5.a presents the evolution of moisture content at the bottom and the surface exposed to air. We observe that an increase of the boundary temperature by 5°C doesn't have any significant impact on the moisture transfer.

Under the same conditions, the gas pressure (figure 5.b) has a peak near the bottom of the plaster due to the initial difference of temperature between the boundary and the plaster.

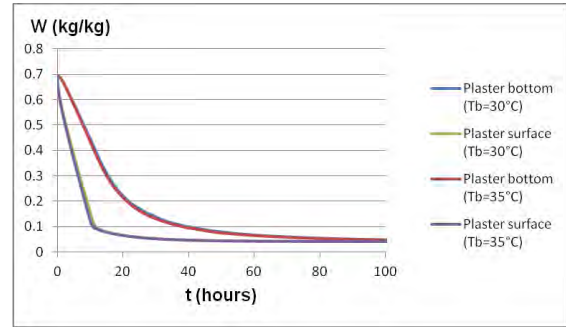


Figure 5.a : Moisture content evolution in the plaster for two tests

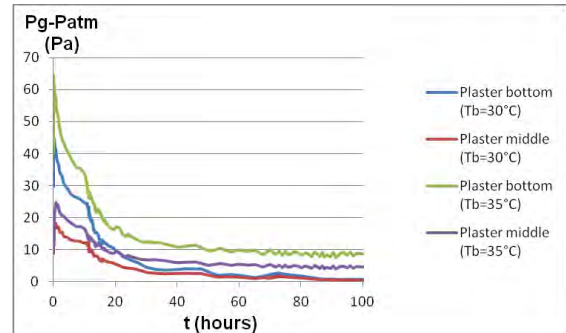


Figure 5.b : Gas pressure evolution in the plaster for two tests

4.3 Multi-layer wall

In the next simulation, we modelize a two-layer wall made of cellular concrete and lime hemp plaster as described in the figure 1. The initial conditions are stated in the table 3. The air has a temperature of 30°C and a relative humidity of 0.5.

	Concrete	Plaster
T (°C)	30	20
W (kg/kg)	0.025	0.3
RH	0.5	1

Table 3 : Initial conditions for multi-layer simulation

4.3.1 Temperature profile

Figure 6 shows the evolution of the temperature profile within the wall between 0 and 20 hours. At $t=0$ hours, there is a step at the interface between the cellular concrete and the lime hemp plaster ($x=0.3\text{m}$) due to the initial conditions. Later, the temperature becomes stationary in the entire wall and have little significant variations after 10 hours.

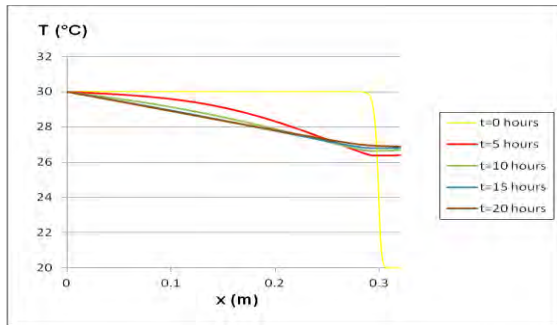


Figure 6 : Temperature profile of the wall at times between 0 and 20 hours

4.3.2 Vapour pressure profile

Figure 7 shows the evolution of the vapour pressure profile within the wall between 0 and 20 hours. Just as the temperature, it has a step at the interface due to initial conditions that lessens after the simulation has started. Vapour pressure increases the first hours due to the temperature elevation, then decreases due to the humidity loss by convective drying.

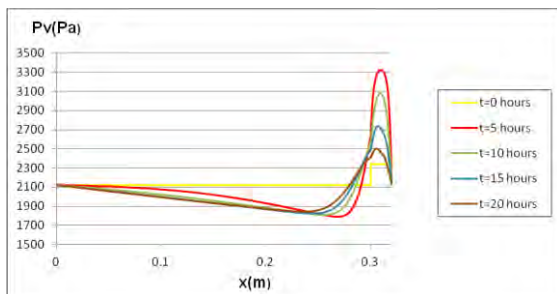


Figure 7 : Vapour pressure profile of the wall at times between 0 and 20 hours

4.3.3 Gas pressure

Similarly to the figure 5.b, a small elevation of gas pressure is observable in the figure 8. It appears in the plaster near the interface with the concrete, because of the initial temperature gradient between the two materials.

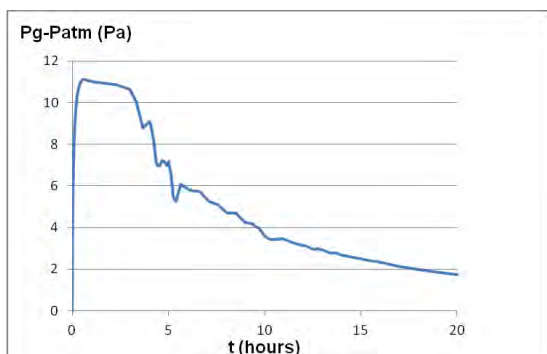


Figure 8 : Gas pressure in the lime hemp plaster layer

4.3.4 Shrinkage

Due to the water transfer from the lime hemp plaster to the air (via evaporation) and the cellular concrete (via diffusion), the thickness of the plaster layer decreases while his apparent density increases (Figure 9).

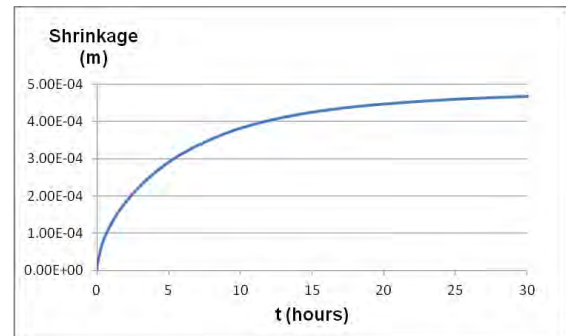


Figure 9 : Shrinkage of the lime hemp plaster layer

5. Conclusion

This system has been developed to modelize the hygrothermal behaviour of a single-layer material as well as a multi-layer wall while solving the discontinuity issues at the interface between two materials. The COMSOL software allowed us to calculate the evolution of temperature, vapour pressure and shrinkage during the drying of wet lime hemp plaster on dry cellular concrete.

6. References

- [1] D.A De Vries, "Simultaneous transfer of heat and moisture in porous media", *Trans Am Geophys Union*, vol.39, p.909-916
- [2] J.R.Philip, D.A.De Vries, "Moisture movement in porous material under temperature gradients", *Trans. Amer. Geo-phys. Union*, 38, p.222.232, 1957
- [3] S. Whitaker, "Simultaneous Heat, Mass and Momentum Transfer in Porous Media : A Theory of Drying", vol.13, p.119-203, Elsevier 1977
- [4] F.Tariku, K.Kumaran, P.Fazio, "Transient model for coupled heat, air and moisture transfer through multilayered porous media ", *International Journal of Heat and Mass Transfer*, vol.53, p.3035-3044, 2010
- [5] M.Qin, R.Belarbi, A.Aït-Mokhtar, L-O.Nilsson, "Coupled heat and moisture transfer in multi-layer building materials", *Construction and Building Materials*, vol.23, p.967-975, 2009

[6] P.Salagnac, P.Glouannec, D.Lecharpentier, "Numerical modelling of heat and mass transfer in porous medium during combined hot air, infrared and microwaves drying", *International Journal of Heat and Mass Transfer*, vol.47, p.4479-4489, 2004

[7] A.Zaknour, "Etude du comportement thermohydrrique de matériaux chanvre-chaux lors de la phase de séchage – Estimation par technique inverse des propriétés hydriques", *PhD Thesis*, 2011

7.Nomenclature

C_p	specific heat capacity (J/K.kg)
D^w	transport coefficient associated to a moisture content gradient (kg/m.s)
D^T	transport coefficient associated to a temperature gradient (kg/m.s)
D^{P_s}	transport coefficient associated to a pressure gradient (kg/m.s)
h_c	convective heat transfer coefficient (W/m ² .s)
ΔH_{ad}	differential heat of sorption (J/kg)
L_v	latent heat of vaporization (J/kg)
M	molar mass (kg/mol)
P	pressure (Pa)
R	ideal gas constant (J/K.mol)
RH	relative humidity (-)
S	liquid saturation (-)
T	temperature (K)
V	velocity (m/s)
W	moisture content (kg/kg)
θ	sorption capacity
λ	thermal conductivity (W/m.K)
ρ	density (kg/m ³)

Subscripts

s	solid
l	liquid
g	gas
a	air
v	vapour
app	apparent

8.Appendix

$$D_l^w = \rho_l \frac{k k_{rl}}{\mu_l} \left(\frac{\partial P_c}{\partial W} \right)$$

$$D_v^w = -D_{v,eff} \left(\frac{M_a M_v}{MRT} \right) \left(\frac{\partial P_v}{\partial W} \right)$$

$$D_a^w = -D_v^w$$

$$D_l^T = \rho_l \frac{k k_{rl}}{\mu_l} \left(\frac{\partial P_c}{\partial T} \right)$$

$$D_v^T = -D_{v,eff} \left(\frac{M_a M_v}{MRT} \right) \left(\frac{\partial P_v}{\partial T} \right)$$

$$D_a^T = -D_v^T$$

$$D_l^{Pg} = \rho_l \frac{k k_{rl}}{\mu_l} \left(\frac{\partial P_c}{\partial P_g} - 1 \right)$$

$$D_v^{Pg} = \rho_v \frac{k k_{rg}}{\mu_g} - D_{v,eff} \left(\frac{M_a M_v}{MRT} \right) \frac{P_v}{P_g}$$

$$D_a^{Pg} = \rho_a \frac{k k_{rg}}{\mu_g} - D_{v,eff} \left(\frac{M_a M_v}{MRT} \right) \frac{P_v}{P_g}$$

$$D_{v,eff} = 4.34 \cdot 10^{-6} k_{rg} \left(\frac{T}{273.15} \right)^{1.88}$$

$$\gamma_1 = \gamma_3 \left[\frac{P_v - P_g}{T} - \frac{\partial P_v}{\partial T} \right]$$

$$\gamma_2 = -\gamma_3 \left[\frac{\partial P_v}{\partial W} - \frac{\rho_s (P_g - P_v)}{\rho_l \epsilon (1-S)} \right]$$

$$\gamma_3 = \frac{\epsilon M_a (1-S)}{RT}$$

$$S = \frac{W \rho_s}{\epsilon \rho_l}$$